Research Article

Fabrication of Au-polymer hybrid colloids via a pH-modulated in situ reduction process for improved catalytic activity

Jing Peng[1,2] · Dongyan Tang[1,2]

Received: 18 September 2022 / Accepted: 5 December 2022
Published online: 16 December 2022

Abstract
Here, we reported a novel strategy for the controllable synthesis of Au nanoparticles within functional microgels. By simply mixing $Au(Cl)_4^-$ ions with a microgel dispersion at room temperature for several hours, Au(III) ions were reduced into Au(0) nanoparticles on the surface of the microgels. Without the use of any additional reductant, the reduction of the Au(III) ions was realized and controlled by tuning the volume of the base solution as a result of the unique reductive 3-carbonyl-*N*-vinylcaprolactam structure inside the microgels. Moreover, the hybrid microgels showed efficient catalytic activities for the model reduction reaction of 4-nitrophenol (Nip). These results revealed that the synthesis strategy of fabricating Au-polymer hybrids possesses great potential in the field of wastewater treatment.

Article highlights

- A novel functional microgel is tailored for the reduction and stabilization of Au(III) into Au nanoparticles.
- The reduction process is switched by adjusting the base volume to generate Au nanoparticles with gradually varied absorption spectra.
- The fabricated Au-polymer hybrids exhibit excellent catalytic activity towards 4-nitrophenol dyes.

Keywords Au nanoparticles · Hybrid microgels · *In situ* synthesis · Dye molecules · Catalytic reduction

1 Introduction

Functional microgels have attracted increasing interest in the nanotechnology field since they are known to have diverse functions in a confined hollow network structure that gives access to load nanoparticles without potential aggregation [1, 2]. These microgels, in which functional groups can be introduced and modified, are usually considered perfect candidates for the stabilization of nanomaterials. Besides, the interaction of the microgels with metal precursors enables the in situ nucleation and growth of nanoparticles in the confined network with controllable valence modulation of metals atoms. Furthermore, the structures and physical properties of functional microgels can be altered at the nanoscale, which opens up an effective route to modulate the optical and catalytic properties of nanoparticles. Therefore, these functional microgels with tailored active groups often act as perfect

Supplementary Information The online version contains supplementary material available at https://doi.org/10.1007/s42452-022-05252-0.

✉ Dongyan Tang, dytang@hit.edu.cn | [1]State Key Laboratory of Advanced Welding and Joining, Harbin Institute of Technology, Harbin 150090, China. [2]School of Chemistry and Chemical Engineering, Harbin Institute of Technology, Harbin 150001, China.

carriers to immobilize nanoparticles for tunable catalysis [3, 4], plasmon sensing [5], surface enhanced Raman scattering [6], and cancer therapy [7, 8].

Au nanoparticles, as one of the most frequently used nanomaterials, have got great achievements in nanotechnology for their remarkable optical and catalytic properties [9–11]. To immobilize Au nanoparticles with a desired size and morphology, a variety of microgels systems [1, 12] have been developed, such as the polystyrene-poly(*N*-isopropylacrylamide) (PS-PNIPAM) core-shell microgels reported by Lu et al. [13] and Fe_3O_4-PNIPAM by Liz-Marzàn et al. [14], both of which were employed to in situ synthesize metal nanoparticles. In these studies, NIPAM offered a weak complexion effect to stabilize the surface of nanoparticles, while $NaBH_4$ was used as a strong reducing agent. Suzuki et al. introduced 3-(methacrylamino)-propyltrimethylammonium chloride into microgels as cationic sites to absorb $[AuCl_4]^-$ anion for further reduction [15]. Pich et al. developed PVCL-based acetoacetoxyethylmethacrylate (AAEM)/acrylic acid core/shell microgels to reduce Au(III) ions in the core in a controllable way. In addition to a strong complexing effect, AAEM also worked as a mild reducing agent for the controlled reduction of Au(III) ions to Au(0) [16, 17], during which acrylic acid played as stabilizer to coordinate with metal atoms [18–20]. Additionally, other microgel systems with α-cyclodextrin (α-CD) used as both reducing agent and stabilizer have also been reported as they often contains plenty of hydroxyl groups [21, 22]. In this study, Au nanoparticles were immobilized by functioning PVCL-based microgels with 3-carbonyl-*N*-vinylcaprolactam units in such a way that the reductive ability of diketone can be modulated by carboxyl groups to produce the pH-modulatable reductive property towards Au(III) ions.

2 Results and discussion

Poly(N-vinylcaprolactam-*co*-3-carbonyl-*N*-vinylcaprolactam) (PTBVCL-d) microgels were synthesized by modified emulsion polymerization (see Supporting Information for details). The reduction reaction of Au nanoparticles was performed in the presence of the as-synthesized microgels. As illustrated in Fig. 1, after Au(III) ions solution was added to the ionized microgel dispersion, the color of the reaction solution changed from colorless to dark violet in 6 h, indicating Au(III) ions were reduced into Au(0) atoms. The diketone formed between caprolactam and the carboxyl groups has been reported to have strong coordination effect and weak reducing ability, resulting in an electron-rich reducing environment via keto–enol tautomerization [17, 23]. During the reduction of Au(III) ion into Au(0), it is believed that the active C-H groups in the diketone structure were oxidized into C-OH groups, similar to the cases of polyol and polyglycidol [17, 24]. The UV-vis absorption spectra obtained at different reaction time in Figure S1a indicate the reduction basically ended in 12 h. These reduction reactions show that the reducing ability of PTBVCL-d microgels is milder than strong reducing agents such as $NaBH_4$ [14], but slightly stronger than reductive polymeric components like α-CD and AAEM [16, 17, 22].

Notably, this reduction process towards Au(III) ions can be controlled by adjusting the amount of NaOH. Figure S1b shows the absorption spectra of a series of Au-polymer hybrids fabricated at different NaOH concentrations. As the volume of NaOH solution (0.1 M) increased from 50 to 200 µL, the absorption peak raised from 530.0 to 542.5 nm. The generation of the absorption peaks was ascribed to the localized surface plasmon reason effect

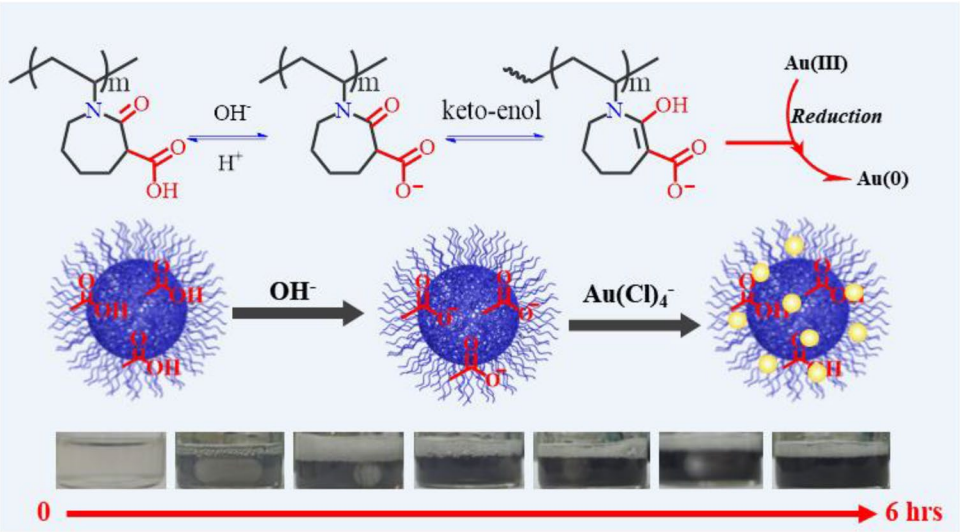

Fig. 1 Schematic diagram of the in situ reduction of Au nanoparticles in the presence of PTBVCL-d copolymer microgels and its color changes as the reduction time increased from 0 to 6 h

in Au nanoparticles; and the redshift implied the formation of Au nanoparticles at lager sizes when the amount of NaOH increased. In the absence of NaOH, however, neither any recognizable color changes nor an absorption peak could be found for the solution even when it had been kept for 3 days.

These results revealed that the addition of NaOH could switch "on/off" the reducing ability of microgels and facilitate the reduction of Au(III) ions into Au(0) colloidal nanoparticles. The switch of such reducing ability by the addition of NaOH may stem from the unique structure of 3-carbonyl-N-vinylcaprolactam. At higher pH values, the carboxyl groups were deprotonated and possessed negative charges that can electrostatically absorb and concentrate Au(III) ions. Besides, ionized carboxyl created an electron-richer reducing environment for the formation of Au nanoparticles. In this sense, increasing the amount of NaOH could obviously alter the reducing ability of microgels, further accelerate the formation of Au nanoparticles, and regulate the plasmon resonance of Au nanoparticles.

Figure 2a, b shows the transmission electron microscopy (TEM) images of PTBVCL-d-Au hybrids microgels. A large amount of spherical colloidal Au nanoparticles localized on the surface of the as-synthesized hybrid microgels were separated from each other as a result of the capping effect of the 3-carbonyl-*N*-vinylcaprolactam units, which was functionally similar to that of cationic surfactants [18, 25]. Based on the calculation from the TEM data (Figure S2), Au nanoparticles have an average size of 6.1 nm. The distribution of Au nanoparticles suggests the formation of Au nanoparticles occurred on the surface of microgels due to the charge repulsion between ionized 3-carbonyl-*N*-vinylcaprolacam units. Besides, almost no aggregation of Au nanoparticles was observed except for few nanocrystals distributed outside the microgels. In consistence with this finding, the dynamic light scattering measurement (Figure S3) prompted the absence of free particles at the nanoscale. These results suggest that there was an effective coordination between 3-carbonyl-*N*-vinylcaprolacam and the surface atoms of Au nanoparticles.

Further structure identification of Au nanoparticles was performed by the high resolution TEM (HRTEM) and selected area electron diffraction (SAED), as presented in Fig. 2c, d. From the HRTEM data, nanocrystals have a

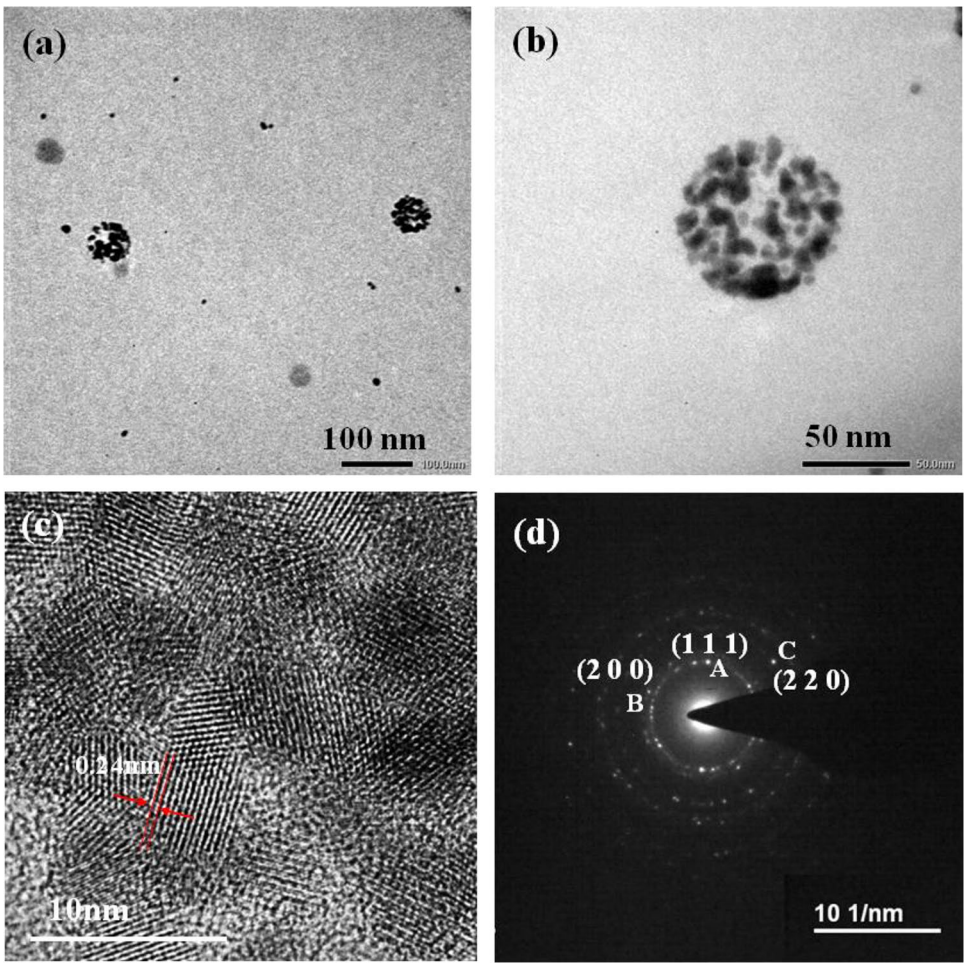

Fig. 2 Low (**a**) and high (**b**) magnification TEM images, HRTEM (**c**) and SAED (**d**) imgages of PTBVCL-d@Au hybrid microgels treated with 50 µL of NaOH solution

polycrystalline structure along with a lattice spacing of 0.24 nm, which was in line with the crystal plane (1 1 1) of Au nanoparticles. In consistence with this result, a similar conclusion was drawn from SAED. The characteristic Bragg peaks from SAED were at 0.24 nm, 0.20 nm and 0.14 nm, corresponding to the (1 1 1), (2 0 0) and (2 2 0) plane of Au nanoparticles, respectively, which in turn matched the result of HRTEM. In addition, thermogravimetric analysis (TGA) has been conducted to measure the content of inorganic/organic component and the result was given in Figure S4. Based on the TGA data, the weight% of Au nanoparticles in hybrids is calculated to be 2.2%, slightly smaller than the theoretical value of 2.3%.

According to previous studies [22, 26], the Nip molecules is a typical pollutant in the field of waste treatment, while it is easy to be detected by UV-vis spectroscopy for further quantitative analysis. Therefore, the catalytic activity of hybrid microgels was evaluated through a common model reaction of Nip reduction by $NaBH_4$. The reduction reaction was performed with PTBVCL-d@Au50 hybrid microgels at different concentrations. Figure 3 shows the kinetics of Nip reduction as the volume of original PTBVCL-d@Au50 hybrid microgels dispersion varied from 25 μL to 100 μL. Correspondingly, the surface area S of Au nanoparticles normalized to the unit volume of the system is calculated to be 3.27×10^{-2} m^2/L, 6.54×10^{-2} m^2/L, 9.81×10^{-2} m^2/L and 1.31×10^{-1} m^2/L, based on the data of size and weight% of Au nanoparticles. The peaks at 400 nm, resulting from the production of 4-nitrophenate ions, experienced a rapid decline as the reaction time decreased, and new minor peaks were observed at 290 nm due to the production of 4-aminophenol. From these curves, it can be observed that the reaction time dropped from about 20 min to 6 min when the amount of hybrid microgels increased. The ratio of the concentration of the Nip at time t to its original concentration can be obtained based on the ratio of the absorbance $A(t)$ to A_0 since the amount of $NaBH_4$ was in excess and a pseudo-first order reaction was followed.

The catalytic activity of hybrid microgels was evaluated by linear relations of $\ln(C/C_0)$ as a function of time, as presented in Figure S5 and Fig. 4a. When the concentration

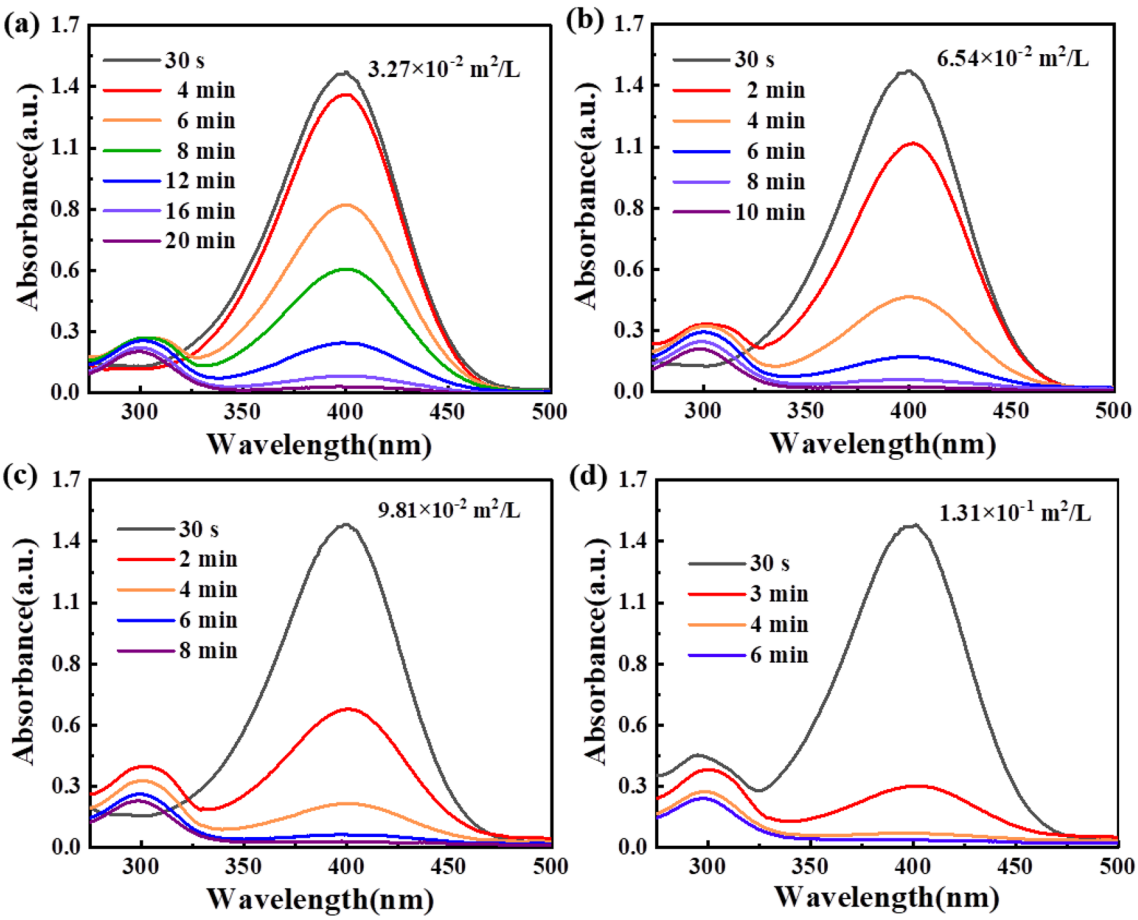

Fig. 3 The UV-vis absorption spectra of Nip reduced by sodium borohydride and catalyzed by **a** 25 μL, **b** 50 μL, **c** 75 μL and **d** 100 μL of PTBVCL-d@Au hybrid microgels (The induction period of the reaction has been **s**ubtracted)

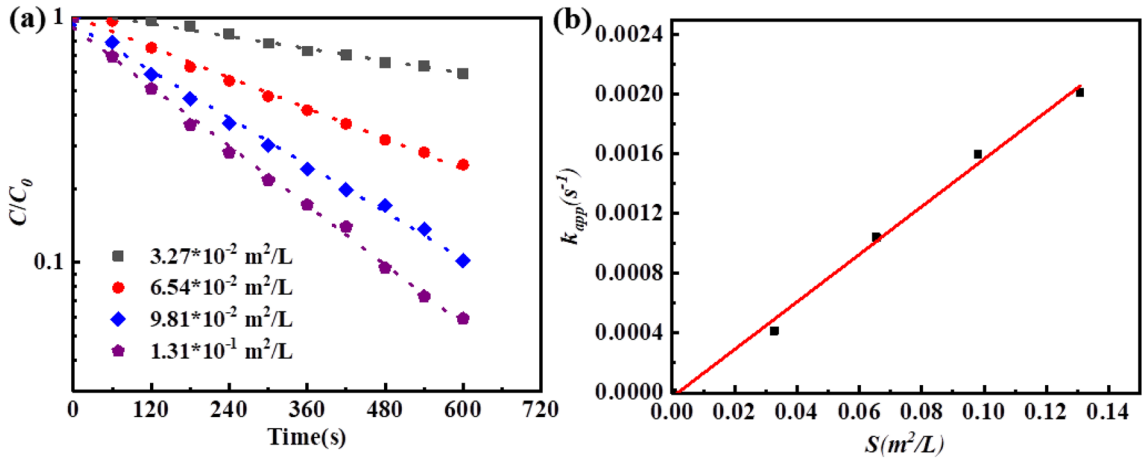

Fig. 4 **a** Kinetic analysis of the Nip reduced by different amounts of PTBVCL-d@Au hybrid microgels (the induction period of the reaction has been **s**ubtracted) and apperent rate constant (k_{app}) as a function of surface area S of Au nanoparticles normalized to the unit volume of the system

of Au nanoparticles reached $1.31 \times 10^{-1} m^2/L$, over 90% of the Nip was converted into 4-nitrophenate in 8 min. The apparent rate constant k_{app} was obtained from the slope of fitting lines. Considering the catalytic degradation only occurred on the surface of Au nanoparticles, the catalytic activity highly depends on the total surface areas of Au nanoparticles in the system. As a result, kinetic constant k_0 can be defined by normalizing the unit of the surface areas of nanoparticles to eliminate the effect of nanoparticle size on the catalysis performance. As presented in Fig. 4b, the normalized rate constant k_0 for PTBVCL-d@Au hybrid microgels was calculated to be 0.016 $Ls^{-1}m^2$. Compared with previous studies, the catalytic activity for PTBVCL-d@Au hybrid microgels is much higher than that of CTAB-stabilized Au ($k_0 = 0.008\ Ls^{-1}m^2$) [22] or Au-loaded porous carbon ($k_0 = 2.76 \times 10^{-4}\ Ls^{-1}m^2$) [27], indicating that PTBVCL-d microgels functioning as reducing agent and stabilizer can effectively facilitate the formation of catalytically active Au nanoparticles. However, this result is lower than that of PVCL-α-CD-Au ($k_0 = 0.025\ Ls^{-1}m^2$) [22], which might be ascribed to a higher amount of active sites of polyhydroxy α-CD than TBVCL to complex with Nip molecules.

The morphology and structure of hybrid microgels after the catalysis experiment are observed through TEM and SAED. As presented in Figure S6a-b, the SAED data shows observable electron diffraction pattern similar to the origin sample, indicating Au nanoparticles after catalysis remained its crystal structure. Besides, plenty of nanoparticles on the surface of microgels can be observed in Figure S6b. These results demonstrate good structural stability of the hybrid microgels in the catalysis process. However, due to the very low concentration at 2.9×10^{-2} mg/mL, the hybrid microgels can hardly be recycled from the catalytic system. Thus, the reusability analysis of hybrid microgels is difficult to evaluate in an operable way. The thermoresponsivity was usually utilized to enable hybrid microgels reusability via reversible thermoresponsive swelling-collapse transition. Here, the thermoresponsive behavior of the hybrid microgels was confirmed by the dynamic light scattering measurement, as shown in Figure S3. In this sense, we believe the hybrid microgels are potentially recyclable in consideration with the similarity of our hybrid structures to those explored in previous studies [20, 28].

3 Conclusion

Briefly, Au-polymer hybrid structures have been successfully fabricated in situ in a mild and controllable process by utilizing the reducing ability of 3-carbonyl-*N*-vinylcaprolactam units in microgels. Besides, this reduction process can be switched is with the usage of base, along with varying absorption spectra. The model reaction of catalysis reduction of Nip molecules demonstrates that the Au-polymer hybrid structures feature highly effective catalytic activity, despite further testing is needed to understand the catalytic mechanism and explore their potential recyclability. These results demonstrated 3-carbonyl-N-vinylcaprolactam units we introduced have excellent ability to interact with metal ions and switch metal valences and fabricate hybrid structures in the nanotechnology. Besides, it is important to note that these hybrid structures may also be applicable to surface enhanced Raman scattering, photothermal therapy and other fields.

Acknowledgements The authors are grateful for the Open Project of State Key Laboratory of Advanced Welding and Joining, Harbin Institute of Technology, China (No. AWJ-22Z01).

Declarations

Conflict of interest There are no conflicts to declare.

References

1. Arif M, Farooqi ZH, Irfan A, Begum R (2021) Gold nanoparticles and polymer microgels: last five years of their happy and successful marriage. J Mol Liq. https://doi.org/10.1016/j.molliq.2021.116270
2. Lee W, Kim D, Lee S, Park J, Oh S, Kim G, Lim J, Kim J (2018) Stimuli-responsive switchable organic–inorganic nanocomposite materials. Nano Today 23:97. https://doi.org/10.1016/j.nantod.2018.10.006
3. Kureha T, Nagase Y, Suzuki D (2018) High reusability of catalytically active gold nanoparticles immobilized in core–shell hydrogel microspheres. Acs Omega 3:6158. https://doi.org/10.1021/acsomega.8b00819
4. Jia H, Cao J, Lu Y (2017) Design and fabrication of functional hybrid materials for catalytic applications. Curr Opin Green Sustain Chem 4:16. https://doi.org/10.1016/j.cogsc.2017.02.002
5. Gao S, Koshizaki N, Tokuhisa H, Koyama E, Sasaki T, Kim J-K, Ryu J, Kim D-S, Shimizu Y (2010) Highly stable au nanoparticles with tunable spacing and their potential application in surface plasmon resonance biosensors. Adv Funct Mater 20:78. https://doi.org/10.1002/adfm.200901232
6. Yan S, An R, Zou YJ, Yang N, Zhang Y (2020) Fabrication of polymer colloidal/au composite nanofilms for stable and reusable sers-active substrates with highly-dense hotspots. Sens Actuators B-Chem. https://doi.org/10.1016/j.snb.2019.127107
7. Wang YT, Wang L, Yan MM, Dong SL, Hao JC (2017) Near-infrared-light-responsive magnetic DNA microgels for photon and magneto-manipulated cancer therapy. ACS Appl Mater Interfaces 9:28185. https://doi.org/10.1021/acsami.7b05502
8. Yoshida A, Kitayama Y, Kiguchi K, Yamada T, Akasaka H, Sasaki R, Takeuchi T (2019) Gold nanoparticle-incorporated molecularly imprinted microgels as radiation sensitizers in pancreatic cancer. Acs Appl Bio Mater 2:1177. https://doi.org/10.1021/acsabm.8b00766
9. Fratoddi I (2018) Hydrophobic and hydrophilic au and ag nanoparticles. Breakthroughs and perspectives. Nanomaterials. https://doi.org/10.3390/nano8010011
10. Ali S, Iqbal M, Naseer A, Yaseen M, Bibi I, Nazir A, Khan MI, Tamam N, Alwadai N, Rizwan M, Abbas M (2021) State of the art of gold (Au) nanoparticles synthesis via green routs and applications: a review. Environ Nanatechnol Monit Manage. https://doi.org/10.1016/j.enmm.2021.100511
11. Jena BK, Ghosh S, Bera R, Dey RS, Das AK, Raj CR (2010) Bioanalytical applications of Au nanoparticles. Recent Pat Nanotechnol 4:41. https://doi.org/10.2174/187221010790712075
12. Farooqi ZH, Khan SR, Begum R, Ijaz A (2016) Review on synthesis, properties, characterization, and applications of responsive microgels fabricated with gold nanostructures. Rev Chem Eng 32:49. https://doi.org/10.1515/revce-2015-0033
13. Lu Y, Mei Y, Drechsler M, Ballauff M (2006) Thermosensitive core–shell particles as carriers for ag nanoparticles: modulating the catalytic activity by a phase transition in networks. Angew Chem Int Ed 45:813. https://doi.org/10.1002/anie.200502731
14. Contreras-Cáceres R, Abalde-Cela S, Guardia-Girós P, Fernández-Barbero A, Pérez-Juste J, Alvarez-Puebla RA, Liz-Marzán LM (2011) Multifunctional microgel magnetic/optical traps for SERS ultradetection. Langmuir 27:4520. https://doi.org/10.1021/la200266e
15. Suzuki D, Nagase Y, Kureha T, Sato T (2014) Internal structures of thermosensitive hybrid microgels investigated by means of small-angle X-ray scattering. J Phys Chem B 118:2194. https://doi.org/10.1021/jp410983x
16. Thies S, Simon P, Zelenina I, Mertens L, Pich A (2018) In situ growth and size regulation of single gold nanoparticles in composite microgels. Small 14:7. https://doi.org/10.1002/smll.201803589
17. Agrawal G, Schuerings MP, van Rijn P, Pich A (2013) Formation of catalytically active gold–polymer microgel hybrids via a controlled in situ reductive process. J Mater Chem A 1:13244. https://doi.org/10.1039/c3ta12370g
18. Liu X-Y, Cheng F, Liu Y, Liu H-J, Chen Y (2010) Preparation and characterization of novel thermoresponsive gold nanoparticles and their responsive catalysis properties. J Mater Chem 20:360. https://doi.org/10.1039/b915313f
19. Choi S, Kim K, Nam J, Shim SE (2013) Synthesis of silica-coated graphite by enolization of polyvinylpyrrolidone and its thermal and electrical conductivity in polymer composites. Carbon 60:254. https://doi.org/10.1016/j.carbon.2013.04.034
20. Satapathy SS, Bhol P, Chakkarambath A, Mohanta J, Samantaray K, Bhat SK, Panda SK, Mohanty PS, Si S (2017) Thermo-responsive PNIPAM-metal hybrids: an efficient nanocatalyst for the reduction of 4-nitrophenol. Appl Surf Sci 420:753. https://doi.org/10.1016/j.apsusc.2017.05.172
21. Zuo YA, Zhao J, Gao YM, Zhang Y (2017) Controllable synthesis of P (NIPAM-co-MPTMS)/PAA–Au composite materials with tunable LSPR performance. J Mater Sci 52:9584. https://doi.org/10.1007/s10853-017-1157-8
22. Jia H, Schmitz D, Ott A, Pich A, Lu Y (2015) Cyclodextrin modified microgels as "nanoreactor" for the generation of au nanoparticles with enhanced catalytic activity. J Mater Chem A 3:6187. https://doi.org/10.1039/c5ta00197h
23. Agrawal M, Pich A, Gupta S, Zafeiropoulos NE, Rubio-Retama J, Simon F, Stamm M (2008) Temperature sensitive hybrid microgels loaded with ZnO nanoparticles. J Mater Chem 18:2581. https://doi.org/10.1039/B802102C
24. Li CC, Cai WP, Cao BQ, Sun FQ, Li Y, Kan CX, Zhang LD (2006) Mass synthesis of large, single-crystal au nanosheets based on a polyol process. Adv Funct Mater 16:83. https://doi.org/10.1002/adfm.200500209
25. Sahiner N (2013) Soft and flexible hydrogel templates of different sizes and various functionalities for metal nanoparticle preparation and their use in catalysis. Prog Polym Sci 38:1329. https://doi.org/10.1016/j.progpolymsci.2013.06.004
26. Kehren D, Pich A (2013) Fabrication and characterisation of microgel/polymer composite microfibres. Macromol Mater Eng 298:1282. https://doi.org/10.1002/mame.201300024

27. Guo J, Suslick KS (2012) Gold nanoparticles encapsulated in porous carbon. Chem Commun 48:11094. https://doi.org/10.1039/C2CC34616H
28. Chen X, Sun J-T, Pan C-Y, Hong C-Y (2015) A facile synthesis of thermo-responsive Au–polymer hybrid microgels through temperature-induced co-aggregation and self-crosslinking. Polym Chem 6:5989. https://doi.org/10.1039/c5py00774g